Molecular Crystals and Liquid Crystals

Publication details, including instructions for authors and subscription information:
http://www.tandfonline.com/loi/gmcl20

A COMPUTER SIMULATION INVESTIGATION OF THE FREEDERICKSZ TRANSITION FOR THE NEMATIC PHASE OF A GAY-BERNE MESOGEN

Geoffrey R. Luckhurst [a] & Katsuhiko Satoh [a]

[a] Department of Chemistry and Southampton Liquid Crystal Institute, University of Southampton, Highfield, Southampton SO17 1BJ, United Kingdom

Version of record first published: 15 Jul 2010

To cite this article: Geoffrey R. Luckhurst & Katsuhiko Satoh (2003): A COMPUTER SIMULATION INVESTIGATION OF THE FREEDERICKSZ TRANSITION FOR THE NEMATIC PHASE OF A GAY-BERNE MESOGEN, Molecular Crystals and Liquid Crystals, 402:1, 85-102

To link to this article: http://dx.doi.org/10.1080/744816840

Mol. Cryst. Liq. Cryst., Vol. 402, pp. 85/[321]–102/[338], 2003

ISSN: 1542-1406 print/1563-5287 online
DOI: 10.1080/15421400390243354

Taylor & Francis
Taylor & Francis Group

A COMPUTER SIMULATION INVESTIGATION OF THE FREEDERICKSZ TRANSITION FOR THE NEMATIC PHASE OF A GAY-BERNE MESOGEN

Geoffrey R. Luckhurst and Katsuhiko Satoh
Department of Chemistry and Southampton Liquid Crystal Institute, University of Southampton, Highfield, Southampton SO17 1BJ, United Kingdom

We present the first computer simulation study of the Freedericksz transition in a nematic phase using a Gay-Berne model mesogen, in which the constituent molecules can both rotate and translate freely. The behaviour and structure of the nematic obtained from the simulation for the Freedericksz transition are compared with those for real nematogens. The twist elastic constant has been estimated directly from the threshold field and found to be significantly larger than for real systems although comparable to another Gay-Berne nematogen. The molecules in the middle of the cell are observed to have a biaxial order in the vicinity of the Freedericksz transition. Those molecules adjacent to the surface are found to be unpinned in a discontinuous transition at a field significantly larger than the threshold field for the Freedericksz transition.

Keywords: nematic; elastic constant; Freedericksz transition; Gay-Berne mesogen; computer simulation

INTRODUCTION

The elastic properties of a nematic liquid crystal provide a clear manifestation of the crystalline nature of the state of matter. In the ground state the director is uniformly aligned but deviations from this state can be created by the application of an external field in conjunction with surface alignment. Alternatively thermal fluctuations are also able to disturb this uniform state because the elastic energy is relatively small. According to the Oseen-Zocher-Frank continuum theory of nematics, there are just three elastic constants which determine the elastic energy needed to create a

We are grateful to the EPSRC for the award of a Postdoctoral Research Fellowship (GR/M38575) to K.S. He also thanks the Anglo-Japanese Daiwa Foundation for financial support and the British Council for a travel grant.

particular director deformation [1]. These are K_1 for the splay deformation, K_2 for the twist and K_3 for the bend deformation. A knowledge of the elastic constants is important in many applications of liquid crystals; for example, they determine, in part, the threshold voltage for display devices. They are also of fundamental importance for, as Frank has noted [2], they provide a route to the anisotropic intermolecular forces which determine liquid crystal behaviour.

There is, however, no direct relationship between the intermolecular potential and the elastic constants. This link can be found with the aid of analytic theories usually based on the molecular field approximation [3]. An alternative route to understanding the relationship between molecular interactions and the elastic constants is to use computer simulation techniques, Monte Carlo or molecular dynamics, to study model mesogenic systems [4]. The extraction of the elastic constants from the simulation data can be achieved using two quite different approaches. In one the formal relationship between the elastic constants and the direct pair correlation function first proposed by Poniewerski and Stecki [5] is used. The other broad approach is to simulate the experiments used to determine the elastic constants for real nematogens [6]. These include the ingenious experiments described by Freedericksz in which surface forces are used to control the director alignment in a thin nematic slab [7]. A magnetic field is then applied to oppose this alignment and the director orientation determined as a function of the field strength. The threshold field at which the director orientation starts to change is directly proportional to the square root of the elastic constant appropriate for the deformation induced by the field. A quite different approach, developed by the Orsay Liquid Crystal group, is based on the thermal fluctuations in the director orientation [7]. As a result of the birefringence of the nematic this causes light to be scattered for different experimental geometries and, perturbed by a field, yields the elastic constants.

All of these approaches have been employed to determine the elastic constants of model nematics but the number of investigations is relatively small [4]. We have, therefore, determined the twist elastic constant for the generic Gay-Berne mesogen, GB(4.4,20.0,1,1) whose properties have been the subject of a detailed investigation [8]. The method used to evaluate K_2 was to simulate the appropriate Freedericksz experiment. In addition to the determination of the twist elastic constant we were also able to explore the molecular organisation in the nematic film and how it changed during the Freedericksz transition as well as at fields higher than the threshold value. The details of the model including the surface used to pin the director together with the details of the Monte Carlo simulation are described in the following section. The results of the simulation and their significance are described in the penultimate section. A summary of our investigation is contained in the final section.

SIMULATION DETAILS

The constant pressure-constant temperature, *NPT*, Monte Carlo technique has been used in this simulation of the Freedericksz transition for the nematic phase for a Gay-Berne mesogen. Thus each molecule can rotate and translate freely, as in a real nematic. The Gay-Berne model potential with a parameter set, $(\kappa, \kappa', \mu, \nu) = (4.4,20.0,1,1)$ namely GB(4.4,20.0,1,1), that has been investigated in detail [8], was used in the simulation. A system of 1728 molecules at a scaled pressure, $P^*(\equiv P\sigma_0{}^3/\varepsilon_0)$, of 2.0 and a scaled temperature, $T^*(\equiv k_B T/\varepsilon_0)$, of 1.65 was used; at this temperature and pressure the mesogen exists as a nematic phase. The two parallel surfaces of the cell were constructed from Gay-Berne molecules with the same parameters as those used for those in the nematic slab; each surface contained 108 particles. The molecules forming the surfaces were fixed on a planar rectangular lattice. Periodic boundary conditions were applied in the *x*- and *y*-directions while the top and bottom surface layers of molecules were aligned with the easy axis for the surface in the x-direction. The *x*- and *y*-dimensions of the cell were allowed to change to maintain a constant pressure, while the *z*-direction corresponding to the cell thickness was held fixed. The external field was applied in the *y*-direction that is orthogonal to the easy axis in the surface. The contribution to the energy from the interaction of the external field with molecule, *i*, is given by

$$U_{\text{ext}} = -\lambda P_2(\cos\theta_i), \tag{1}$$

where θ_i is the angle between the symmetry axis for the *i*th molecule and the external field vector which we take to be a magnetic field. λ is the strength parameter for the anisotropic magnetic interaction and is given by

$$\lambda = \Delta\kappa B^2/3\mu_0, \tag{2}$$

where $\Delta\kappa$ is the anisotropy in the molecular magnetic polarizability, and μ_0, is the vacuum permeability. In the simulation, a scaled strength parameter, $\lambda^*(\equiv \lambda\ 3\mu_0/\Delta\kappa B^2\varepsilon_0)$ was used. The second rank orientational order parameter was determined via

$$Q_{\alpha\beta} = N^{-1}\sum_i (3u_\alpha^i u_\beta^i - \delta_{\alpha\beta})/2, \tag{3}$$

where u_α^i is the component, $\alpha = x$, y or z, of the unit vector giving the orientation of the symmetry axis for molecule i and N is the number of particles in the nematic slab. The second rank orientational order parameter, $\langle P_2\rangle$, was determined from the maximum eigenvalue which was

obtained by diagonalizing the $\mathbf{Q}$-tensor, its eigenvector is then identified as the director. The translational order parameter was estimated via

$$\tau = |\exp(2i\pi x^*/d^*)|. \quad (4)$$

This definition is independent of the choice of the origin for the x^*-coordinates. However, it is necessary to know the scaled periodicity of the smectic phase. The value of $d^*(\equiv d/\sigma_0)$ was estimated by finding the value which maximized τ. This maximum value was identified as the translational order parameter.

In order to probe the molecular organisation within the system in detail, some properties were determined as a function of the z^*-coordinate, that is the distance across the slab. Each slice has a width δz^* of 2.0. The quantity $(Q_{xx}^{lab}\text{-}Q_{yy}^{lab})$ using the $\mathbf{Q}$-tensor expressed in the laboratory frame can be thought of as a biaxial order parameter. It does, however, reflect the extent to which the director is rotated in the xy-plane. In this study, the variation of the structure was investigated as a function of the field strength parameter at a fixed temperature and then as a function of temperature in zero field. Typically 2.0×10^5 cycles were taken for statistical averages after equilibration, and between 4.0×10^5 and 2.0×10^6 cycles were used for equilibration.

RESULTS AND DISCUSSION

The phase behaviour as a function of temperature for this thin slab of mesogen is considered first in order to discuss the difference in behaviour to that for the bulk system. The second rank orientational order parameter, $\langle P_2 \rangle$, and the enthalpy together with the corresponding quantities for the bulk system are shown in Figure 1; the values for the bulk system are in good agreement with those obtained by Bates and Luckhurst [8]. The temperature dependence was obtained from the simulation on cooling. The slab basically exhibits the same phase sequence as that for the bulk system. However, the nematic-isotropic transition for the thin slab system was not so sharp as that for the bulk. This is in accord with the prediction of a molecular field theory for a lattice model [9]. Thus the properties are found to change more and less continuously. The inhomogeneous effective field originating from the interaction with the perfectly ordered molecules constituting the two surfaces has clearly broadened the transition although the orientational order below the nematic-isotropic transition is comparable to that of the bulk system.

The scaled nematic-isotropic transition temperature, T_{NI}^*, which was estimated from the temperature dependence of the change in enthalpy is 1.78. This value is about 0.1 lower than that for the bulk, which also illustrates the influence of the inhomogeneous surface field on the

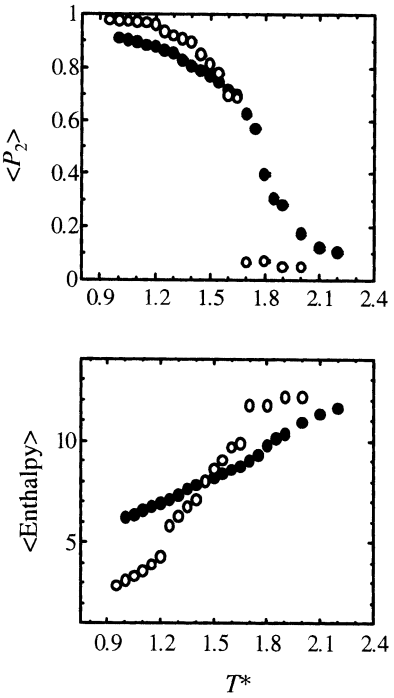

FIGURE 1 Temperature dependence of the second rank orientational order parameter, $\langle P_2 \rangle$, and the enthalpy at $P^* = 2.0$. The closed circles are for the thin slab system used in this study, open circles are for the bulk.

transitional properties. Indeed the change of enthalpy at the transition is 25% smaller than that for the bulk system, and the volume of the isotropic phase at T^* of 2.0 was 7% smaller than that for the bulk mesogen. In addition, it can be seen, from the results in Figure 1, that the value of $\langle P_2 \rangle$ was non-zero, 0.17, even at T^* of 2.0. This confirms that the system has been ordered locally because of the inhomogeneous surface field, as we can see from the dependence of the order parameter, $\langle P_2 \rangle$, on the z^*-coordinate at T^* of 2.0 shown in Figure 2. The molecules in the centre of the cell are found to be orientationally disordered. However, those molecules near the surfaces clearly have an orientational order due to the interaction with the perfectly aligned molecules constituting the surface. The induced order originating from the surface is seen to extend to z^* of *ca.*4.0 even in the isotropic phase. This surface-induced orientational order clearly influences a significantly higher fraction of the sample than for a real system which is necessarily considerably thicker than for that studied here. Next we characterize the nematic formed in the cell at T^* of 1.65, before showing

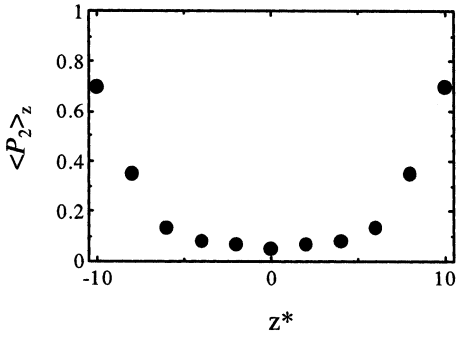

FIGURE 2 The order parameter, $\langle P_2 \rangle_z$, as a function of the z*-coordinate in the isotropic phase at $T^* = 2.0$.

the results for the Freedericksz transition. The density profiles as a function of the x^*- and z^*-coordinates as well as the longitudinal positional pair correlation function, $g_{\parallel}(r^*_{\parallel})$, are shown in Figure 3. Here $r^*_{\parallel}$ is the separation between two molecules projected onto the easy axis. This longitudinal correlation function provides a measure of whether a layer structure is formed or not. The density profiles, $\rho(x^*)$ and $\rho(z^*)$, are the singlet translational distribution functions; x^* and z^* denote the positions of the centre of mass of molecules along the easy axis and along the surface normal, respectively. A periodicity in these distributions would indicate that a layer structure had been formed. Weak periodicities are seen in $g_{\parallel}(r^*_{\parallel})$ and $\rho(x^*)$ due to the interactions with the surface (see the insets in these figures in Figure 3). However, there were apparently no correlations in the middle of the cell in the profile, $\rho(x^*)$, and $g_{\parallel}(r^*_{\parallel})$ which were taken from the centre of the cell (with a thickness of $8\sigma_0$). The singlet distribution function, $\rho(z^*)$, exhibits three sharp peaks with decreasing intensity which result from the interaction with the surfaces; there is, however, no oscillation in the middle of the cell showing the expected homogeneous nature of the system. Thus it would seem that the system forms a nematic phase with its characteristic translational disorder except near to the surfaces.

One method which we have used to determine the threshold field for the Freedericksz transition was to monitor the orientation of the director at the centre of the cell where the influence of the surfaces is weakest. This angle was determined from the $\mathbf{Q}$-tensor evaluated for a thin slice of nematic at the centre of the slab. The resulting dependence of the director orientation with respect to the easy axis on λ^* is shown in Figure 4. It can be seen that the angle begins to increase when λ^* is 0.04. Then the angle increases gradually as λ^* is increased further. The director can be seen to be aligned essentially parallel to the field when λ^* reaches 0.16. To determine the

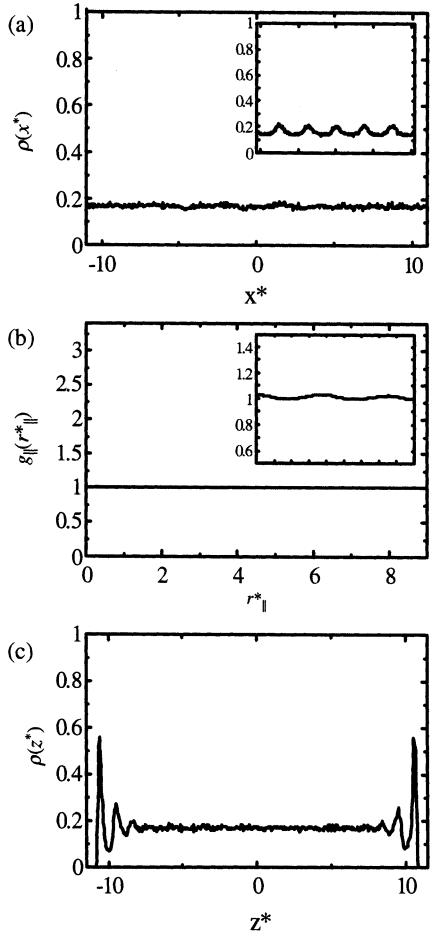

FIGURE 3 (a) The density profile as a function of the x^*-dimension, $\rho(x^*)$, (b) the longitudinal pair correlation function, $g_{||}(r^*_{||})$, and (c) the density profile as a function of the z^*-coordinate, $\rho(z^*)$ for the central region of the cell at $T^* = 1.65$. The insets in figures, (a) and (b), indicate the same profile and correlation function for all of the molecules in the cell.

optimum value of the threshold field we have fitted the data to the continuum theory prediction of θ_m, namely

$$(\lambda/\lambda_{th})^{1/2} = (2/\pi)K(\sin\theta_m), \tag{4}$$

where $K(\sin\theta_m)$ is the complete elliptic integral of the first kind [10]. The results are shown for three values of λ_{th} as the solid dotted and dashed lines in Figure 4; comparing these with the simulation data suggests that

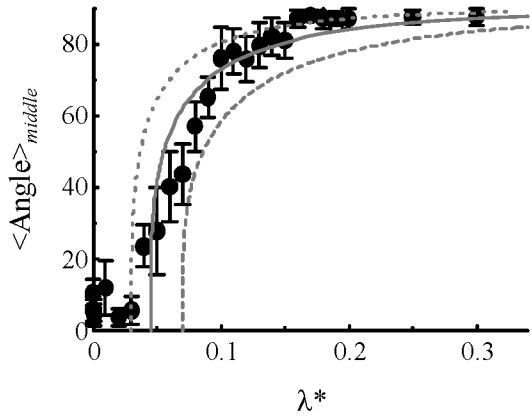

FIGURE 4 The angle made by the director in the middle of the nematic slab with the easy axis as a function of the field strength parameter, λ*, at $T^* = 1.65$. The continuum theory predictions are shown for $\lambda^*_{\rm th}$ of 0.030 (dotted), 0.045 (solid), and 0.070 (dashed).

the optimum value for λ_{th} is 0.045. We note that the angle made by the director at the cell centre was not zero even below λ^* of 0.04 presumably because of thermal fluctuations or the relatively small system size. Cleaver and Allen have also observed a non-zero value for the angle in the middle of the cell below the threshold field for the Lebwohl-Lasher lattice system [11]. However, the Freedericksz transition is clearly seen for GB(4.4,20.0,1,1) although the angle did not change as sharply with the field strength as that predicted by continuum theory [10].

An alternative method of monitoring the Freedericksz transition is to take snapshots of configurations from the production run. These are shown for a selection of field strengths, λ^*, in Figure 5. For λ^* of 0.005, which is below the Freedericksz transition, the molecules are, on average, essentially uniformly aligned parallel to the easy axis, as expected. The other values of λ^* are notionally above the threshold, however for λ^* of 0.070 although the molecules in the centre of the slab have rotated, the remainder especially those at the surface, are still parallel, on average, to the easy axis. This shows that the magnetic coherence length for this field strength is only just comparable to the thickness of the slab. At the significantly higher value for λ^* of 0.15 the molecules in the centre of the slab are essentially parallel to the field but close to the surface the molecules remain parallel to the easy axis. The magnetic coherence length has clearly decreased but is still not negligible in comparison with the thickness of the film. This limit is, however, reached for λ^* of 0.20 when it is apparent that the director is aligned parallel to the field throughout the nematic slab.

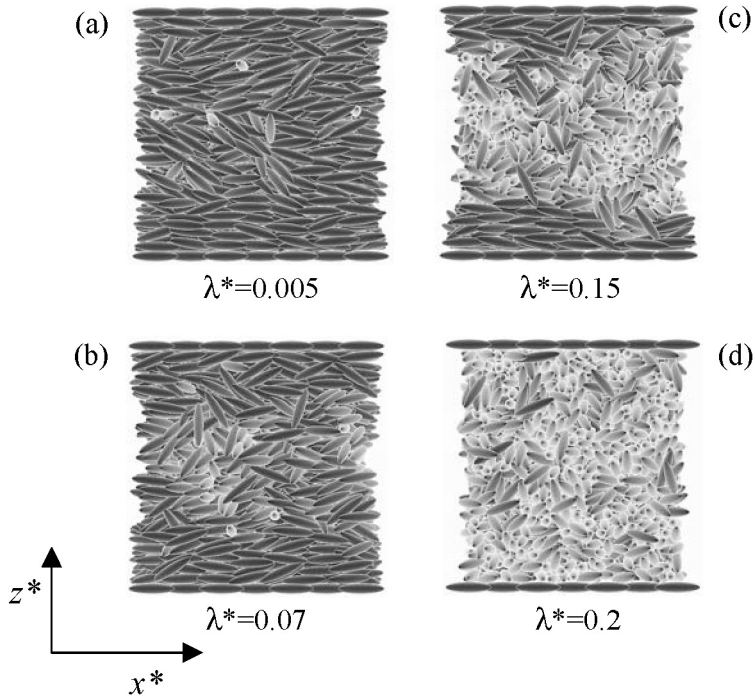

FIGURE 5 Snapshots of configurations in the nematic phase taken at $T^* = 1.65$ for λ* of (a) 0.005, (b) 0.07, (c) 0.15 and (d) 0.20.

Although the snapshots show the major changes which occur to the molecular organisation in the nematic slab on increasing the field strength through the Freedericksz transition they do not provide a quantitative estimate of the threshold strength parameter. However, one way in which the behaviour of the entire nematic can be used to determine the threshold value of λ^* is to mimic the experiments used to obtain this threshold. Since it is difficult to monitor the director orientation in the centre of a thin nematic slab a laboratory component of some tensorial properties, such as the dielectric constant, is determined for the entire film. This component varies with the director orientation integrated over the thickness of the nematic slab. We have also used this approach to determine the threshold field for our system by evaluating the components of the $\boldsymbol{Q}$-tensor along the x- and y-directions of the simulation box.

The values for $\langle \boldsymbol{Q}_{xx} \rangle^{lab}$ and $\langle \boldsymbol{Q}_{yy} \rangle^{lab}$ are shown in Figure 6 as a function of the scaled field strength parameter, λ^*. As we have seen the director is aligned parallel to the x-direction before the transition, then the external

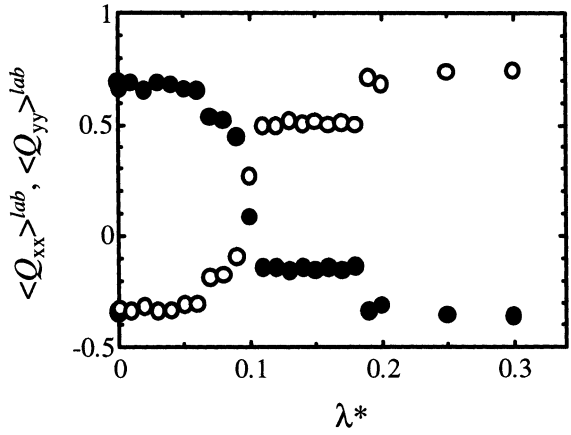

FIGURE 6 The components of the Q-tensor, $\langle Q_{xx}{}^{lab}\rangle$, $\langle Q_{yy}{}^{lab}\rangle$, as a function of the strength of the field, λ^*, at $T^* = 1.65$ in the nematic phase. The closed circles are for $\langle Q_{xx}{}^{lab}\rangle$, open circles are for $\langle Q_{yy}{}^{lab}\rangle$.

field is applied along the y-direction. As the director moves from being parallel to the x-direction to the y, $\langle Q_{xx}\rangle^{lab}$ will alter from being positive to being negative and $\langle Q_{yy}\rangle^{lab}$ will change in the opposite manner. At $\lambda^* = 0.0$, the values of $\langle Q_{xx}\rangle^{lab}$ and $\langle Q_{yy}\rangle^{lab}$ were 0.61 and -0.31, respectively as expected for a uniaxial phase. As λ^* is increased $\langle Q_{xx}\rangle^{lab}$ decreases and $\langle Q_{yy}\rangle^{lab}$ increases gradually corresponding to the alignment of the director away from the easy axis and parallel to the field. Then these values change more rapidly for λ^* between 0.06 and 0.07; the subsequent values exhibit a marked discontinuity when λ^* is between 0.18 and 0.19. It is tempting to attribute the onset of the rapid change in $\langle Q_{xx}\rangle^{lab}$ and $\langle Q_{yy}\rangle^{lab}$ for λ^* between 0.07 and 0.08 with the Freedericksz transition. The fact that this is higher than that determined from the director orientation in the centre of the film obtains because the majority of molecules which contribute to the Q-tensor have not moved (see Figure 5). In other words the Q-tensor is necessarily less dependent on the change in the director orientation at the centre of the nematic slab which provides a more sensitive method with which to locate the Freedericksz transition. The origin of the second jump in the x- and y-components of the Q-tensor is more difficult to interpret especially as it is not predicted by the continuum theory. However, it seems likely that it originates from the alignment of the molecules close to the surface from being parallel to the easy axis to being parallel to the field. Again this dramatic, discontinuous change in the orientation of the molecules at the surface can be seen from the snapshots shown in Figure 5.

In principle the field can also increase the orientational order of the nematic phase as well as changing the director orientation. To see if this has occurred the major order parameter, $\langle P_2 \rangle$, calculated from the $\boldsymbol{Q}$-tensor is shown as a function of the scaled field strength, λ^*, in Figure 7. We see that up to the first jump in $Q_{xx}{}^{lab}$ and $Q_{yy}{}^{lab}$ there is a slight decrease in $\langle P_2 \rangle$ which we attribute to the competition between the surface and field interaction which are orthogonal to each other. There is then a discontinuous decrease in $\langle P_2 \rangle$ which we again attribute to the competition between surface and field as more of the molecules are aligned parallel to the field. As we shall see this results in a biaxiality in the system which is consistent with the reduction in the major order parameter. Then when λ^* is approximately 0.18, $\langle P_2 \rangle$ begins to increase quite rapidly corresponding to the alignment of the director associated with all of the molecules in the slab parallel to the magnetic field. Further increase in the strength of the field causes a small increase in the major order parameter, as expected.

Given the clear formation of domains across the slab during the transition process, it is of interest to examine the structure and its variation in detail. To do this the biaxial order parameter for the phase at the middle of the cell was estimated. This parameter was defined as the difference between the minor eigenvalues of the $\boldsymbol{Q}$-tensor. The field strength dependency of the biaxial order parameter is shown in Figure 8. It starts to increase at essentially the same point as the director orientation in the middle of the cell starts to rise (see Figure 4). The biaxial order parameter then passes through a maximum when λ^* is about 0.07, it returns to approximately zero corresponding to the uniaxial nematic when λ^* is about

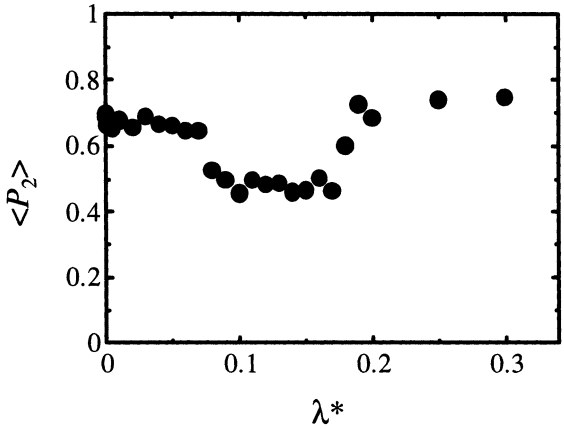

FIGURE 7 The orientational order parameter, $\langle P_2 \rangle$, as a function of the field strength parameter, λ^*, at $T^* = 1.65$.

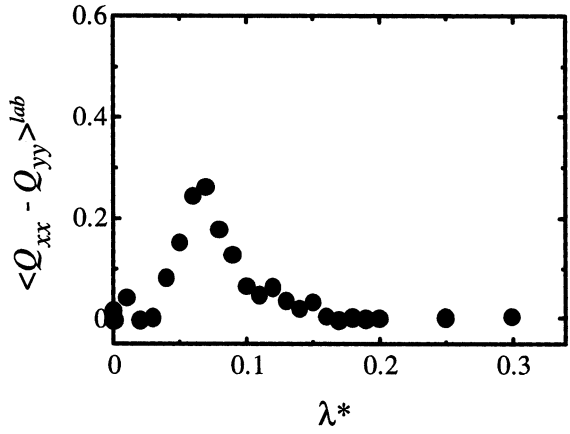

FIGURE 8 The biaxial order parameter in the middle of the nematic slab as a function of the field strength, λ^*, at $T^* = 1.65$.

0.16. The phase has, therefore, biaxial order during the Freedericksz transition resulting from the competition for the molecular orientations coming from the field and surface interactions which have caused different parts of the system to have the molecules aligned orthogonal to each other. However, the continuum theory of the Freedericksz transition assumes that the nematic phase is always uniaxial locally. Consequently, this result suggests that the biaxial behaviour should be considered when the Freedericksz transition is studied for relatively small systems as in our simulations. As far as we are aware the phase biaxiality has not been included in the continuum theory of the transition.

In Figure 9 we show the dependence of the major order parameter $\langle P_2 \rangle$ on the z^*-coordinate for different values of the scaled field strength, λ^*. The orientational order of most regions except near the surfaces are *ca.*0.65 before the transition; for instance at λ^* of 0.01. At the surface $\langle P_2 \rangle$ is large and then decreases to about 0.6 in the centre of the slab. This higher orientational order at the edge of the film clearly originates from the interaction with the perfectly ordered molecules constituting the surface. There is little change to the order parameter profile as the field strength increases to 0.02, 0.04 and 0.05 but at 0.06 the major order parameter at the centre of the cell begins to decrease slightly which is associated with the increase in the biaxial order (see Figure 7). Then when λ^* is 0.07 the order parameter in the middle of the film begins to increase and, as the order parameter at the surface is large, the profile shows a double minimum as well as the maximum in the centre. The maximum grows and the minima deepen as λ^* increases further to 0.08, 0.11 and 0.15. Then at λ^* of 0.20 the layers of molecules at the surface are unpinned and the associated director

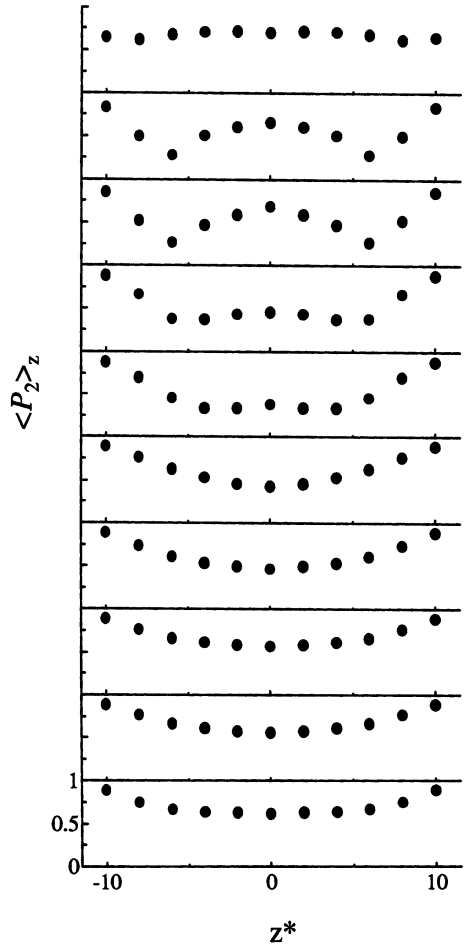

FIGURE 9 The dependence of the orientational order parameter, $\langle P_2 \rangle$, on the z^*-coordinate. At different values of the field strength parameter λ^* from the bottom: 0.01, 0.02, 0.04, 0.05, 0.06, 0.07, 0.08, 0.11, 0.15 and 0.20.

is aligned parallel to the field. At this point the orientational order parameter is essentially uniform across the cell and equal to that for the bulk nematic. Similar variations in the major order parameter across a nematic slab during the Freedericksz transition have also been observed for the Lebwohl-Lasher lattice model [4,6].

The variation of the director orientation across the nematic slab for different field strengths is also available from the simulations and the results are shown in Figure 10. For the field strength parameter, λ^*, of 0.05, 0.07,

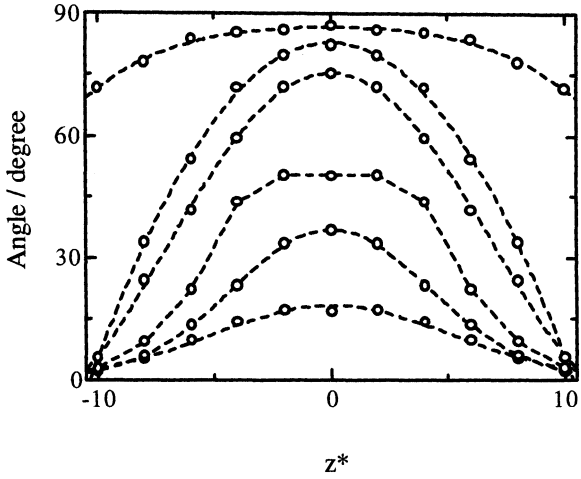

FIGURE 10 The angle made by the director with the easy axis as a function of the z^*-coordinate at various field strengths. The parameter, λ^*, takes values from the bottom: 0.01, 0.05, 0.07, 0.11, 0.15 and 0.20.

0.11 and 0.15 the director at the surface is pinned parallel to the easy axis but in the centre of the slab the angle made by the director with the easy axis grows will increasing field. For λ^* of 0.15 it reaches a value of about 82° corresponding to the alignment of the director almost parallel to the field. Such behaviour is to be expected and is consistent with the predictions of continuum theory [1]. However, for the field strength parameter of 0.20 there is a dramatic change in how the director orientation changes across the slab (see Figure 10). Now the director at the surface is no longer parallel to the easy axis but is essentially parallel to the field and this alignment for the director continues across the nematic slab. Presumably at some critical value of λ^* the field energy exceeds the surface anchoring energy and the director is unpinned from the surface by the field; this is certainly [12] anticipated by continuum theory but not perhaps in the dramatic manner which we have discovered for the Gay-Berne mesogen.

Finally, we turn to the evaluation of the twist elastic constant for GB(4.4,20.0,1,1) from our results for the Freedericksz transition. As we have seen the director orientation at the centre of the nematic slab provides the most sensitive property with which to determine the threshold field parameter, $\lambda^*_{\rm th}$. This is found to be approximately 0.045 and according to the continuum theory the scaled twist elastic constant, $K_2{}^*(\equiv K_2\sigma_0/\varepsilon_0)$ is related to the scaled threshold field by [7]

$$K_2{}^* = 3\lambda^*{}_{\rm th} d^{*^2}\langle P_2\rangle/\pi^2, \tag{5}$$

where d^* is the scaled thickness of the cell which is 20. This gives a value for K_2^* of 4.7. This and values of the twist elastic constants for other systems both real and model are given in the Table 1. There are few values of the twist elastic constant for Gay-Berne nematics which are available and certainly none for the mesogen GB(4.4,20.0,1,1) [4]. The simulations by Stelzer *et al.* [13] used the direct correlation function to estimate all three elastic constants and found a value of 2.7 ± 0.2 for K_2^*. This value is certainly similar to that which we have determined; however, it is clearly important for the results to be compared under analogous conditions. This raises the question as to what these conditions might be. For example, it is found both experimentally and theoretically that the elastic constants are proportional to $\langle P_2 \rangle^2$ [7] and it this dependence which results in the strong temperature variation of the elastic constants. It might be argued, therefore, that the appropriate point of comparison would be for nematics with the same orientational order as reflected by $\langle P_2 \rangle$. Indeed the order parameter for the system we have studied, namely 0.64, is comparable to that for the Gay-Berne nematic investigated by Stelzer *et al.* [12]. However, states of equal order parameter can be obtained by varying the temperature and making compensating changes in the density. Allen *et al.* [14] have determined the elastic constants for the nematic phase of GB(3.0,5.0,2,1) at a selection of such states of essentially equal order parameter and found a significant variation in the elastic constants. For example, when ρ^* is 0.32 and T^* is 0.90 the scaled twist elastic constant is 0.676 ± 0.0055 but at the higher scaled density and temperature of 0.38 and 3.00, respectively K_2^* has increased significantly to 2.53 ± 0.012. This clearly shows that a

TABLE 1 The Twist Elastic Constant K_2 for Two Gay-Berne Mesogens and a Range of Real Mesogens

	T/T_{NI}	K_2^*	$K_2/10^{-12}$ N	$\langle P_2 \rangle$
GB(4.4,20.0,1,1)[this work]	0.930	4.7	33.7	0.64
GB(3.0,5.0,2,1) [12]	–	2.7	19.4	0.65
		5.0	35.9	0.70
GB(3.0,5.0,2,1) [13]	–	0.7	5.0	0.67
		2.5	17.9	0.73
PAA [15]	0.970	–	3.8	–
MBBA [16]	0.928	–	4.0	–
DIBAB [17]	0.967	–	3.0	–
5CB [18]	0.942	–	4.4	–
6CB [18]	0.960	–	3.5	–
7CB [18]	0.943	–	5.4	–
8CB [18]	0.970	–	5.0	–
M2 [19]	0.89	–	7.1	–

comparison of different systems at the same value of $\langle P_2 \rangle$ is not sufficient. The results obtained by Allen *et al.* [14] are, of course, comparable with those obtained for the same Gay-Berne mesogen studied by Stelzer *et al.* [12] but determined via the direct correlation function. At the same state point the value for K_2^* obtained by Stelzer *et al.* [13] is 2.5 ± 0.2 which is about 3.5 times larger than that determined by Allen *et al.* [14] using the spectrum of director fluctuations.

As we have seen there is considerable difficulty in comparing our results for K_2^* with those obtained for other Gay-Berne mesogens. This problem is compounded by the fact that the relative dimensions, κ, of the particles are different so that a comparison at the same number density is not appropriate. A more relevant quantity would be the volume fraction, that is the total volume of the particles divided by that for the system. This quantity is not well-defined for the soft Gay-Berne particles but may be approximated by $(\pi/6)\kappa\rho^*$. For the system we have studied, with its more anisotropic particles, the volume fraction is 0.37 whereas that for GB(3.0,5.0,2,1) studied by Allen *et al.* [14] varies from 0.60 to 0.50. The value for GB(4.4,20.0,1,1) is somewhat smaller than that investigated by Allen *et al.* [13] but since they find that K_2^* decreases with decreasing number density this suggests that for GB(3.0,5.0,2,1) K_2^* should be smaller than 0.676 at the same volume fraction as that which we have studied. Our value for K_2^* is significantly larger at 4.7 although the two model mesogens are significantly different in terms of both the shape and the attractive anisotropies. Clearly further studies of GB(4.4,20.0,1,1) and other Gay-Berne mesogens are needed to confirm our result and to explore the variation of elastic constants with the state variables as well as the anisotropies, κ and κ'.

It is also possible to compare the results of the simulation for the scaled twist elastic constant with those of real nematics provided the scaling parameters, σ_0, and ε_0, are known. These have been estimated for the nematogen, 4, 4′-dimethoxyazoxybenzene(PAA), and found to be $\sigma_0 = 4.5 \times 10^{-10}$ m and $N_A\varepsilon_0 = 2.19$ kJmol^{-1}[8]. This particular nematogen was chosen because it is semi-rigid and its shape approximates to that of a Gay-Berne particle. The elastic constants have been determined for PAA as a function of temperature and at the same reduced temperature, T^*/T^*_{NI} ($\equiv T/T_{NI}$) of 0.930 used in our simulations K_2 is found to 4.3×10^{-12} N. This compares with the unscaled value for GB(4.4,20.0,1,1) of 34×10^{-12} N which is significantly larger than that found for PAA. We should also note that at similar reduced temperatures, the twist elastic constant does not vary significantly with molecular structure as we can see from the results given in the table. However, it is of interest to note that K_2 reported for M2 is somewhat higher than for the other nematogens, this may result because M2 contains three rings and the others have just two. In this connection we

recall that the parameters analogous to those for GB(4.4,20.0,1,1) were obtained by mapping the Gay-Berne potential onto that for *para*-terphenyl modelled atomistically with Lennard-Jones potentials [20]. It is tempting to conclude from our single result as well as those obtained by Stelzer *et al*. [13] and Allen *et al*. [14] that the elastic constants for Gay-Berne mesogens are larger than those of real nematics. However, it may only be reasonable to draw this conclusion if the volume fractions for the different systems were similar.

SUMMARY

We have presented the results of a simulation of the Freedericksz transition in the nematic phase of the model mesogen formed by GB(4.4,20.0,1,1), whose constituent molecules can rotate and translate freely. The structure of the nematic phase was monitored during the Freedericksz transition and found to pass through a biaxial state as a consequence of the interactions of the molecules with the surface and field which are orthogonal constraints. From the threshold field for the transition the scaled twist elastic constant has been estimated together with its absolute value. The value of K_2 for the Gay-Berne mesogen was significantly larger than those of real nematogens although the origins of this difference is not yet understood but could be related to the high pressure of the system. However, K^*_2, which we have determined is similar to that for another Gay-Berne mesogen, GB(3.0,5.0,2,1).

REFERENCES

[1] de Gennes, P. G. & Prost, J. (1993). *The Physics of Liquid Crystals*, Clarendon Press: Oxford.
[2] Frank, F. C. (1958). *Disc. Faraday Soc.*, *25*, 19.
[3] Nehring, J. & Saupe, A. (1971). *J. Chem. Phys.*, *54*, 337.
[4] Cleaver, D. J. (2001). In: *The Physical Properties of Liquid Crystals: Nematics*, Dunmur, D. A., Fukuda, A. & Luckhurst, G. R. (Eds.), INSPEC, IEE: London, Chapt. 12.4.
[5] Poniewerski, A. & Stecki, J. (1979). *Mol. Phys.*, *38*, 1931.
[6] Simpson, P. (1983). Ph.D thesis, University of Southampton.
[7] de Jeu, W. H. (1980). *Physical Properties of Liquid Crystalline Materials*, Gordon and Breach: New York.
[8] Bates, M. A. & Luckhurst, G. R. (1999). *J. Chem. Phys.*, *110*, 7087.
[9] Schroder, H. (1977). *J. Chem. Phys.*, *67*, 16.
[10] Sauper, A. (1960). *Z. Naturforsch., A15*, 815.
[11] Cleaver, D. J. & Allen, M. P. (1991). *Phys. Rev.*, *A43*, 1918.
[12] Sugimura, A., Luckhurst, G. R., & Ou-Yang, Z. (1995). *Phys. Rev.*, *E52*, 681; Sugimura, A., Miyamoto, T., Tsuji, M., & Kuze, M. (1998). *Appl. Phys. Lett.*, *72*, 329.
[13] Stelzer, J., Longa, L., & Trebin, H.-R. (1995). *J. Chem. Phys.*, *103*, 3098.

[14] Allen, M. P., Warren, M. A., Wilson, M. R., Sauron, A., & Smith, W. (1996). ***J. Chem. Phys.***, ***105***, 2850.
[15] Madhusudana, N. V., Karat, P. P., & Chandrasekhar, S. (1975). In: ***Proc. Bangalore Liq. Cryst. Conf.*** Pramana, Suppl. No. 1, p. 225.
[16] Leenhouts, F., van der Woude, F., & Dekker, A. J. (1976). ***Phys. Lett.***, ***58***A, 242.
[17] de Jeu, W. H. & Claassen, W. A. P. (1977). ***J. Chem. Phys.***, ***67***, 3705.
[18] Dunmur, D. A. (2001). In: ***The Physical Properties of Liquid Crystals: Nematics***, Dunmur, D. A., Fukuda, A. & Luckhurst, G. R. (Eds.), INSPEC, IEE: London, Chapt. 5.2.
[19] Saito, H. (2001). In: ***The Physical Properties of Liquid Crystals: Nematics***, Dunmur, D. A., Fukuda, A. & Luckhurst, G. R. (Eds.), INSPEC, IEE: London, Chapt. 11.3.
[20] Luckhurst, G. R. & Simmonds, P. S. J. (1993). ***Mol. Phys.***, ***80***, 233.